IEICE TRANSACTIONS

on Electronics

DOI:10.1587/transele.2024DII0005

Publicized:2024/09/03

This advance publication article will be replaced by the finalized version after proofreading.

A PUBLICATION OF THE ELECTRONICS SOCIETY

The Institute of Electronics, Information and Communication Engineers
Kikai-Shinko-Kaikan Bldg., 5-8, Shibakoen 3chome, Minato-ku, TOKYO, 105-0011 JAPAN

INVITED PAPER

Designing Super-High-Resolution Liquid-Crystal Devices for Electronic Holography Based on Lateral Electric-Field Driving

Hiroto Tochigi†, Masakazu Nakatani[a)†], Ken-ichi Aoshima††, Mayumi Kawana††, Yuta Yamaguchi††, Kenji Machida††, Nobuhiko Funabashi††, *Nonmembers, and* Hideo Fujikake†, *Fellow*

ABSTRACT

In this study, we introduce a lateral electric-field driving system based on continuous potential-difference driving using lateral transparent electrodes to achieve a wide viewing zone angle in electronic holographic displays. We evaluate light modulation to validate the independent driving capability of each pixel at a high resolution (pixel pitch: 1 μm). Additionally, we demonstrate the feasibility of two-dimensional driving by integrating the driving and ground electrodes.

Keywords: electronic holographic display, spatial light modulator, liquid crystals on silicon, phase hologram

1. Introduction

Three-dimensional (3D) displays with depth view heighten the perceptions of presence and realism when viewing images [1]. Technologies, such as 3D movies and stereoscopic TVs, are being considered in the development of the next-generation displays [2]. Among these services, electronic holographic displays are attracting attention as next-generation stereoscopic display systems because of their capacity to replicate the wavefront of object light, thereby displaying natural stereoscopic vision for humans.

In electronic holography, a device, i.e., a spatial light modulator (SLM), is used to replicate the wavefront of object light. Additionally, light diffraction by SLMs is used to recreate an electronic holographic image. Liquid crystal on Silicon (LCOSs) SLMs[3][4], which can only modulate the light phase, are generally used SLMs. This study focuses on phase-modulation-type LCOS SLMs.

The practical application of electronic holography is thwarted by its limited viewing-zone-angle range over which an image can be observed. This angle is determined by the diffraction angle of SLMs, which is also influenced by the pixel pitch constituting SLMs in their two-dimensional (2D) plane. The equation relating the viewing angle and pixel pitch is shown below [5].

$$\psi = 2\sin^{-1}\left(\frac{\lambda}{2p}\right) \qquad (1)$$

The corresponding graph is depicted in Fig. 1. A pixel pitch of 1 μm is required to achieve a viewing zone angle of 30 degrees, which is fit for the human's effective field of view.

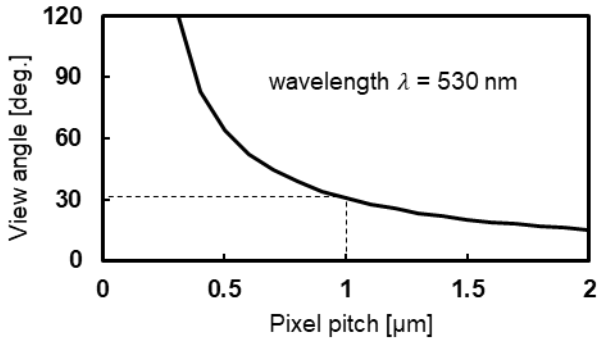

Fig. 1 Relationship between the viewing zone angle and pixel pitch

Meanwhile, a pixel pitch of 0.8 μm results in a wider viewing zone angle of 38 degrees.

However, the realization of the independent driving of each pixel becomes challenging at a pixel pitch of 1 μm in a LCOS SLM because of electric-field leakage from neighboring pixels. Fig. 2 shows the electric field at a pixel pitch of 1μm. In the conventional method, a vertical electric field is applied perpendicularly to the substrate for easy manufacturing. However, in this setup, the electric field extends radially over a small area, resulting in substantial electric-field leakage to neighboring pixels. This paper is organized as follows. Section 2 described related works to this research. Section 3.1 describes 1D simulation at a pixel pitch of 1 μm. Section 3.2 discusses 1D electric-field driving. Section 3.3 presents 1D simulation at a pixel pitch of 0.8 μm, and Section 4 describes 2D simulation.

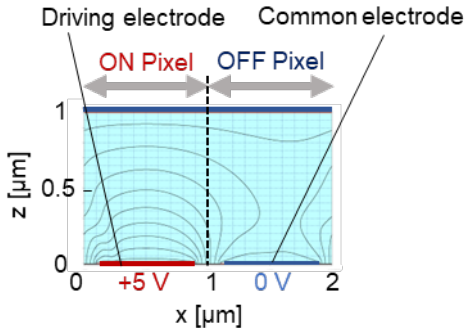

Fig. 2 Vertical electric-field driving at a pixel pitch of 1μm.

a) masakazu.nakatani.b5@tohoku.ac.jp

†Department of Electronics, Graduate school of Engineering, Tohoku University, Sendai, 980-8579 Japan.

††The author is with NHK, Setagaya-ku, Tokyo, 157-8510 Japan.

2. Related works

Liquid-crystal driving systems in direct-viewed liquid-crystal displays include virtual alignment (VA) LC cells [6], twisted nematic (TN) LC cells [7], super twisted nematic (STN) LC cells [8], in-plane switching (IPS) LC cells [9], and dielectric shield structures [10]. Among these, VA LC, TN LC, and STN LC cells fail to address the leakage problem. The dielectric shield wall structure features a two-dimensional arrangement of lattice-shaped dielectric walls along pixel boundaries at a pitch pixel of 1 μm. These walls effectively suppress electric-field leakage and enable the independent driving of each pixel. However, these dielectric walls must be precisely aligned along the pixel grid, rendering the implementation of this approach challenging by precise pasting.

In an IPS LC cell, the electric-field spread is smaller than that in a vertical-field driving when applying a voltage of the same magnitude, as shown in Fig. 3. Therefore, employing a lateral electric-field driving can suppress electric-field leakage, thereby potentially enabling the construction of an LCOS SLM structure with a pixel pitch of 1 μm without requiring dielectric walls for suppressing electric-field leakage. To date, there has been no report of SLMs using a lateral electric-field driving for the LCOS SLM, and this will be explored in this study.

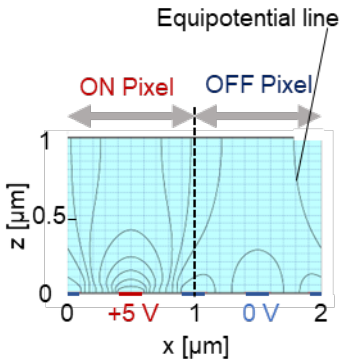

Fig. 3 IPS driving at a pixel pitch of 1μm.

Unlike the in-plane rotation employed in IPS for yielding a phase-modulated LCOS SLM, the lateral electric-field driving aligns liquid-crystal molecules vertically on the substrate. Conventional IPS driving uses the electric field generated by an absolute voltage, called absolute-voltage driving, as shown in Fig. 4(a). However, in the absolute-voltage driving, the driving electrode at the center of the pixel applies an electric field toward the common electrode at the pixel boundary, which prevents alignment change and phase modulation over the driving electrode center. Thus, the center of the driving electrode becoming no-modulation area. To address this, we propose a potential difference driving system based on continuous potential-difference driving using lateral electrodes, as shown in Fig. 4(b). In potential difference driving, the driving electrodes are positioned at the pixel boundary, rather than common electrodes. By applying continuous voltage, each driving electrode generates an electric field using the potential difference, as shown in Fig. 4(c). The potential difference driving method requires fewer electrodes than conventional methods, making it conducive for higher-resolution displays.

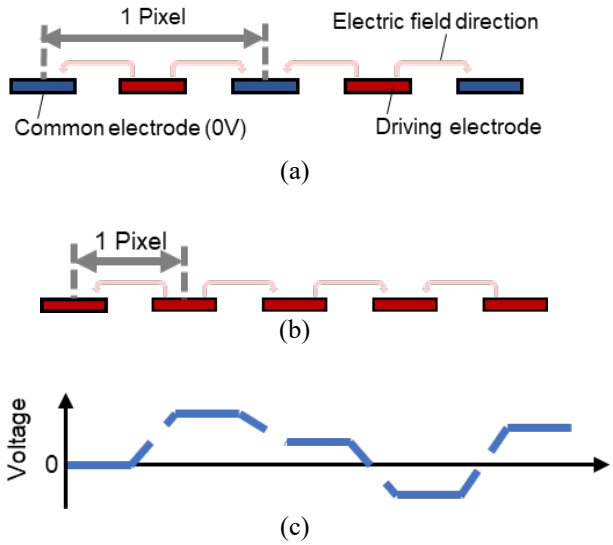

Fig. 4 Absolute-voltage and potential difference driving methods. (a) Absolute-voltage driving used in direct display. (b) Potential difference driving. (c) Potential difference driving potential

Yang, etc. proposed a 1D driving method, wherein the top and bottom electrodes are sandwiched between a ground electrode for reduce leakage[11]. This approach effectively suppresses electric-field leakage. Similarly, we proposed a 2D driving method that combines the potential difference driving mechanism with a ground electrode to suppress electric-field leakage. The plane of ground and driving electrode in xy direction is depicted in Fig. 5. This method constitutes our initial proposal. With this structural enhancement, we anticipated that pixels could be arranged in a 2D plane with a pixel pitch of 1 μm and independently driven. 2D driving by potential difference driving and ground electrode method constitutes our initial proposal

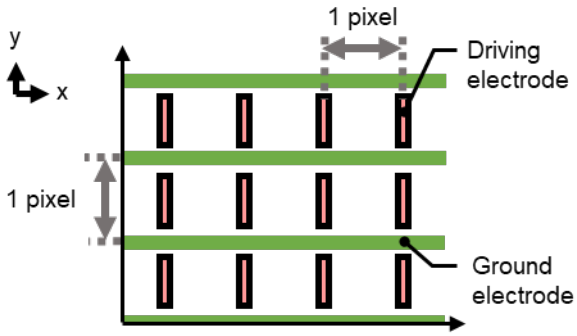

Fig. 5 Electrode arrangement using the lateral electric-field driving system based on continuous potential-difference driving by employing lateral electrodes

3. Lateral electric-field system based on continuous potential-difference driving using lateral electrodes

3.1 Simulation analysis of the proposed structure at a pixel pitch of 1 μm

The amount of phase modulation required in phase-modulation electron holography is 2π; however, in the case of a reflective SLM, modulating π in one direction in phase-modulation electron holography is sufficient as the light travels back and forth. In our proposed lateral electric-field driving using a continuous potential difference, we utilized a liquid-crystal material, ZOC-A1015XX (supplied by JNC Corporation in Japan; $\Delta n = 0.5$, $\Delta \varepsilon = 19.5$), because an ideal liquid-crystal material exhibits a small electric-field spread as well as large refractive-index and dielectric-constant anisotropies. The thickness of the liquid-crystal layer required to ensure sufficient phase modulation, π, is 2 μm.

Based on the foregoing, we examined how a lateral electric field is driven based on a continuous potential difference at a liquid-crystal layer thickness of 2 μm and at a pixel pitch of 1 μm. For verification, we performed numerical simulations using the liquid-crystal-alignment calculation software (LCD Master, Shintech in Japan) based on the elastic body theory of liquid crystals. We discussed the results based on the simulation and driving as below.

Fig. 6 shows the simulation structure, wherein OFF electrode is shown in dark blue, ON electrode is denoted in dark red, OFF pixel is represented in light blue, and ON pixel is shown in light red. To confirm the independent driving of each pixel, pixels that are driven to obtain a phase modulation of 0 (OFF pixels) and those that are driven to obtain a phase modulation of π (ON pixels) are arranged alternately. To configure potential difference, The driving electrodes comprising the OFF and ON pixels are set to the same potential and a potential difference, respectively. The width of the driving electrodes and that between the electrodes are 0.2 and 0.8 μm, respectively. When driven under these conditions, we investigated whether the required amount of phase modulation could be secured in each pixel and whether each pixel could be driven independently.

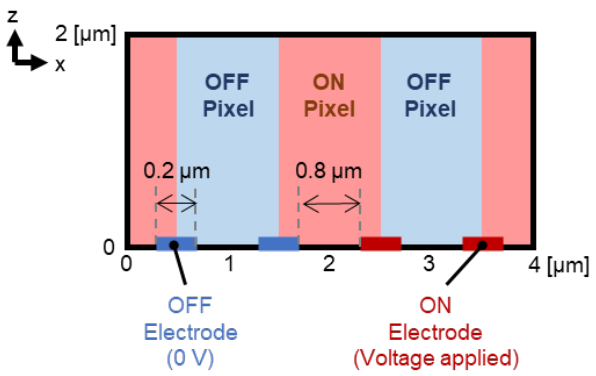

Fig. 6 Simulation structure

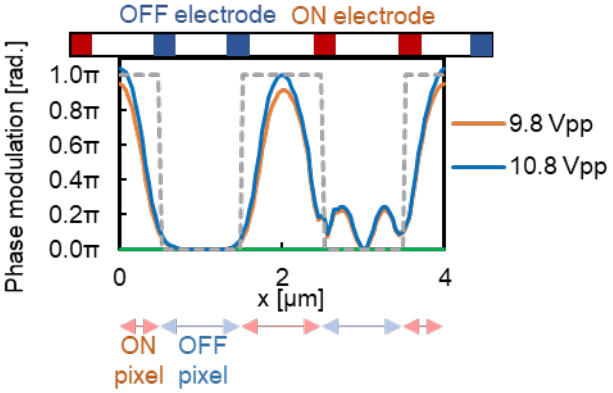

Fig. 7 Analysis results of phase-modulation distribution

The phase-modulation distribution for each pixel was displayed as a simulation result. Fig. 7 shows the phase-modulation distribution for the proposed structure at a pixel pitch of 1 μm. ON and OFF pixels generated by the electrode potential difference are depicted in the upper region of Fig. 7, with the corresponding electrodes demonstrated above them. This figure shows that π-phase modulation is achieved with the ON pixel at a potential difference of 10.8 Vpp and depicts a state with a potential difference of 9.8 Vpp, corresponding to 10% lower voltage than 10.8 Vpp. It can be seen that a difference in phase modulation by π is realized between the ON and OFF pixels. Additionally, low-phase modulation occurs near the region where the ON electrode and OFF pixel overlap. However, this phase modulation is smaller than that at the ON pixel. Conversely, no phase modulation occurs at the region where the OFF electrode and OFF pixel are in contact. Each pixel can be driven independently with sufficient phase modulation.

The simulation results reveal that the application of the continuous potential-difference lateral electric-field driving can ensure phase modulation by a sufficient amount at a pixel pitch of 1 μm and that the independent driving of each pixel is possible.

3.2 Resolution evaluation of the 1 μm pixel pitch driving

To evaluate the independent driving of each pixel in the lateral electric-field driving method based on a continuous potential difference at a pixel pitch of 1 μm shown in the simulation, liquid-crystal elements were fabricated, and their polarizing microscopy images were observed. Liquid-crystal devices to be fabricated are devices employing the lateral electric-field driving method based on a continuous potential difference and a device utilizing the conventional vertical-field driving method; both comprise a one-dimensional (1D) fine-pixel electrode.

Fig. 8 shows the structure of fabricated liquid-crystal devices. Fig. 8(a) depicts the vertical electric-field driving mechanism, while Fig. 8(b) illustrates the potential

difference driving mechanism under a lateral electric field. Notably, the absolute-voltage driving was not measured here owing to a no-modulation area at the top of the electrode. Two electrode lines connected to each terminal were extended to a lower electrode substrate in the potential difference driving method by employing a continuous potential difference. The electrode lines extending from the same terminal could also produce an OFF pixel. Conversely, electrode lines extending from different terminals have a potential difference, which produces an ON pixel. An elementary glass substrate was used as the upper substrate. In the substrate for vertical-field driving, the electrode lines connected to each terminal were alternately lined in a stripe pattern. Further, the area above the electrodes was becomed as a pixel, with the ON and OFF pixels being arranged in alternating rows. Additionally, the upper substrate was an all-electrode substrate fabricated using indium tin oxide as the electric field was applied vertically to the substrate.

Light modulation was observed with liquid-crystal devices, and we evaluated their resolution. Bright and dark lines appeared when the independent driving of each pixel was realized. However, these lines blurred out when independent driving was not realized. Fig. 9 shows the results of the observation of the fabricated liquid-crystal device under a polarizing microscope at a wavelength of 500 nm. Bright and dark lines were observed in the liquid-crystal device driven by a continuous potential difference under a lateral electric field (Fig. 9(a)), confirming the significance of independent driving. Contrarily, for a liquid-crystal device driven by the vertical electric field (Fig. 9 (b)), the bright and dark lines were blurred and independent driving of the pixels was not achieved.

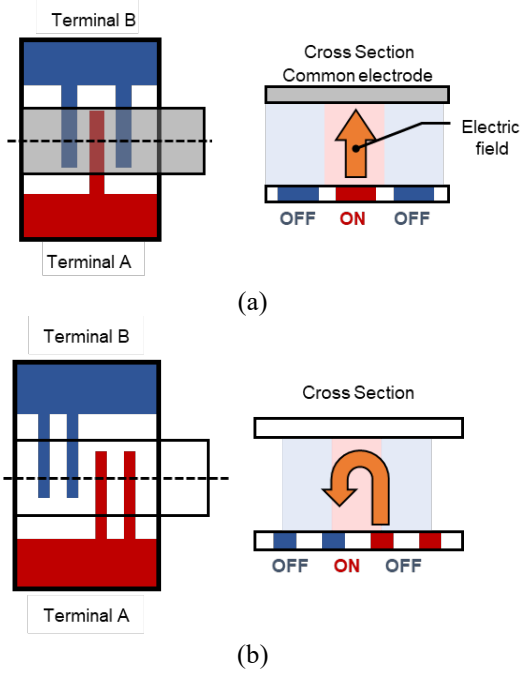

Fig. 8 Structure of liquid-crystal devices to be fabricated: (a) vertical and (b) lateral electric-field driving using a continuous potential difference

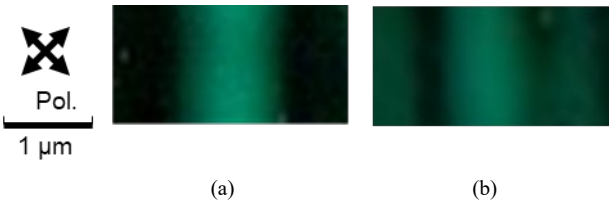

Fig. 9 Cross-Nicol arrangement results: (a) potential difference driving under a lateral electric field (applied 10.8 Vpp) and (b) vertical electric-field driving (applied 5 Vpp)

To quantitatively evaluate the results of this polarizing microscope observation, we introduced a parameter called modulation as an evaluation index [9]. By calculating the distribution of luminance values on a straight line orthogonal to the alternating bright and dark lines and taking P_{max} and P_{min} as the maximum and minimum luminance values in the modulation area, respectively, the maximum modulation degree, M_{max} , was calculated using the following equation (1):

$$M_{max} = \frac{P_{max} - P_{min}}{P_{max} + P_{min}}. \qquad (1)$$

The larger the achieved independent liquid-crystal driving, the closer the M_{max} value to 1. By calculating the modulation degree at each electrode pitch, the independence of the pixel pitch and liquid-crystal driving was examined. M_{max} = 0.90 and 0.59 for the lateral- and vertical-field-driving liquid-crystal devices, respectively, indicate that high modulation characteristics were realized using the lateral electric-field driving based on a continuous potential difference.

3.3 Simulation analysis of the proposed structure at 0.8-μm pixel pitch

In Subsection 3.2, we examined driving at a pixel pitch of 1 μm using the lateral electric-field driving based on a continuous potential difference. Here, we evaluated driving at a pixel pitch of ≤1 μm by simulating the lateral electric-field driving based on a continuous potential difference.

Fig. 10 shows the simulation structure. Similar to the simulation at a pixel pitch of 1 μm, a voltage was applied in the structure with alternating ON and OFF pixels, and the amount of phase modulation was evaluated.

Fig. 11 shows the simulation results, indicating that the required amount of phase modulation can be secured per pixel at the pixel pitches of 0.8 and 1 μm. At present, we decided on a pixel pitch of 0.8 μm because it could be fabricating precision limiting of fine electrode and each pixel could be independently driven. In the simulation, the voltage applied at the 0.8 μm pitch to obtain the phase-modulation amount, π, was higher than that applied at the 1 μm pixel pitch. The increase in the required applied voltage was attributed to an increase in the elastic resistance of the liquid crystal due to the narrowed electrode width such as a pixel pitch of 0.8 μm.

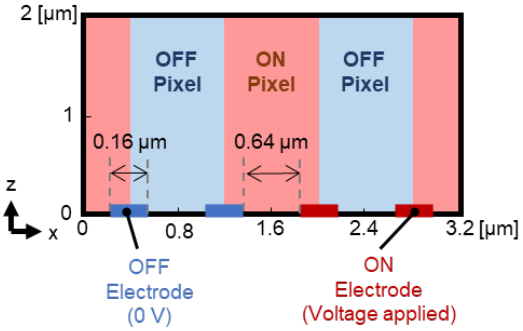

Fig. 10 Simulation structure

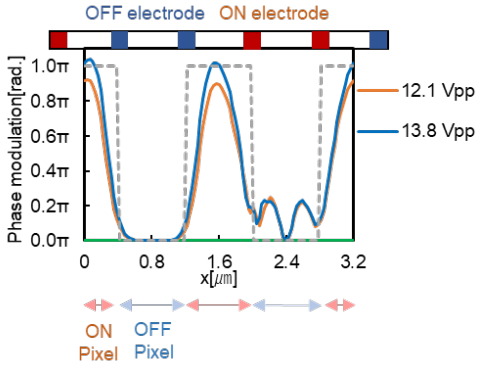

Fig. 11 Analysis results of the phase-modulation distribution

Based on the foregoing, simulations revealed that each pixel could be independently driven at a pixel pitch of ≤1 μm using lateral electric-field driving based on a continuous potential difference.

4. Suppression of electric-field leakage using ground electrode

In Section 3, we demonstrated the usefulness of lateral-field driving based on a continuous potential difference in driving pixels at a pixel pitch of ≤1 μm. Although, the discussion in Section 3 was based on a 1D pixel structure, actual SLMs exhibit 2D pixel structures. Electric-field leakage can still occur between voltage applied rows and no voltage applied rows even if a 2D-pixel structure was fabricated by arranging one row of continuous potential difference–based lateral electric-field driving in 1D, followed by the arrangement of rows. In other words, independent driving becomes complicated in 2D-pixel arrangements. Therefore, it is necessary to obtain a structure that suppresses electric-field leakage between rows. In this study, we proposed the installation of ground electrodes between rows, and in this section, we discuss the usefulness of these electrodes.

To verify 2D pixel by simulation, a structure that combines the lateral electric-field driving based on a continuous potential difference and a ground electrode was used. To verify the electric-field-shielding effect achieved by the ground electrode, we simulated structures with and without the ground electrode (Figs. 10 (a) and (b)). The phase-modulation and potential-orientation distributions per structure were obtained from the simulation and are illustrated in Fig. 12. The driving electrode in the middle row was voltage applied for driving alternate OFF and ON pixels. Therefore, voltage was applied to the two driving ON electrodes on the right, and 0 V was applied to the two driving OFF electrodes on the left. As pixels in the upper and lower rows were OFF pixels, 0 V was applied to the driving electrodes. The parameters of each electrode are described below, and the observation plane is given as follows: to obtain the phase-modulation distribution of surrounding OFF pixels, an observation was made regarding the XZ plane of the cross-section at two driving ON electrodes (y_1) that are crossed. This XZ plane was designated as the observation cross-section {1}. Next, the phase-modulation distribution of the XZ plane of the cross-section at the upper row (y_2) was observed to determine the required applied voltage to obtain the leakage of phase modulation. This XZ plane was designated as the observed cross-section {2}. Thereafter, the potential-orientation distribution in the XY plane at Z = 0.5 μm (z_1) was observed to investigate the electric-field spread within the device plane. This XY plane was designated as the element in-plane observation plane {3}.The device plane was set at Z = 0.5 μm because this is the height at which the orientation change in liquid-crystal molecules tended to be enormous. The independent driving of each pixel could be realized by suppressing electric-field leakage in this plane.

First, simulations were conducted considering a pixel pitch of 1 μm. The parameters were set as follows: y_{gap} = x_{gap} = 1 μm, y_1 = 1.5 μm, and y_2 = 2.5 μm. The driving electrodes measured 0.2 and 0.6 μm along the X and Y directions, respectively. Meanwhile, the width of the ground electrode was 0.2 μm.

Figs. 13 and 14 show the simulation results based on the foregoing regarding 1-μm simulation. Applied voltages at which a sufficient amount of phase modulation could be obtained from the observed cross-section {1} were 10.8 and 8.6 V with and without the ground electrodes, respectively (Fig. 13(a)). The applied voltage was higher with the ground electrode condition because the ground electrode is closer to the driving electrode and voltage is tend to suppressed for enough to phase modulation. The two structures with and without the ground electrodes were compared when this voltage was applied. The phase-modulation distribution within the observed cross-section {2} is depicted in Fig. 13(b), while that within the phase modulation bar expanded cross-section {2} is depicted in Fig. 13(c). Without the ground electrode, the maximum phase modulation was 0.062π. Conversely, with the ground electrode, the maximum phase modulation was reduced to 0.023π. Thus, leakage is suppressed in this case using a ground electrode. As illustrated in Fig. 14(a), in the presence of the ground electrode, the electric potential does not spread to the upper and lower rows of the element in the in-plane observation

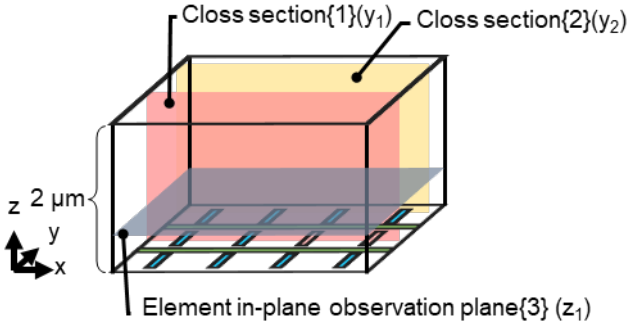

(a)

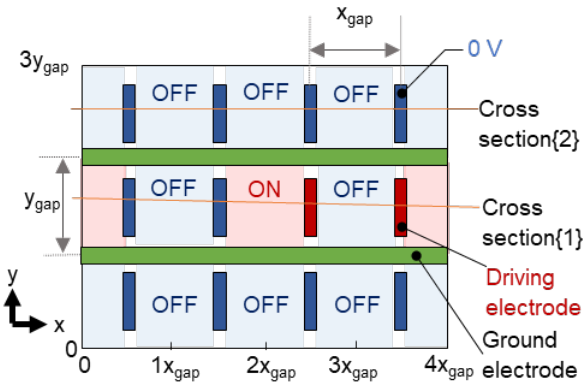

(b)

Fig. 12 Simulation structure: (a) view along diagonally above and (b) ground plan

plane {3}. As depicted in Fig. 14(a), the ground electrode positioned 0.5 μm above the electrode suppresses potential, resulting in a lower potential. Conversely, as illustrated in Fig. 14(b), without the ground electrode, the electric potential spreads to the upper and lower rows. Thus, the ground electrode achieves leakage suppression within the element in the in-plane observation plane.

The foregoing simulation discussion revealed the possibility of independent driving for pixels at a pixel pitch of ≤1 μm in 2D using a structure that combines lateral-field driving based on a continuous potential difference with a ground electrode.

Next, the 0.8-μm pitch simulation was performed. Here, the parameters were $y_{gap} = x_{gap} = 0.8$ μm, $y_1 = 1.2$ μm, and $y_2 = 2$ μm. The driving electrodes measured 0.16 and 0.48 μm in the X and Y directions, respectively. The width of the ground electrode was 0.16 μm.

Figs. 15 and 16 show the simulation results based on the foregoing. Applied voltages at which sufficient amounts of phase modulation could be obtained from the observed cross-section {1} were 13.8 and 11 V with and without the ground electrodes, respectively (Fig. 15(a)). The applied voltage was higher at the ground electrode condition because the ground electrode is closer and voltage is suppressed. Fig. 15(b), and phase modulation bar expanded cross-section {2} is shown in Fig. 15(c). The maximum phase modulation without the ground electrode was 0.077π,

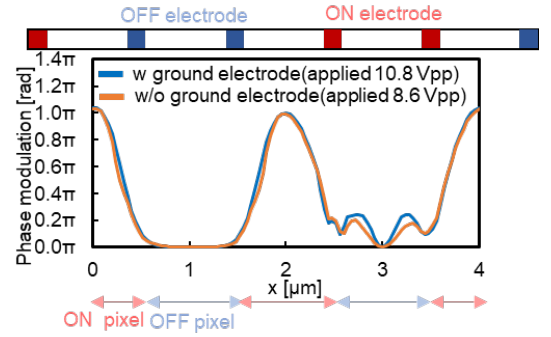

(a)

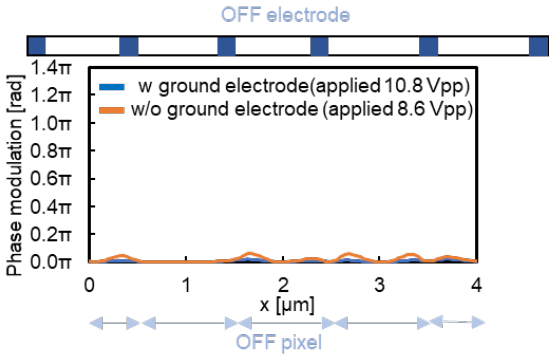

(b)

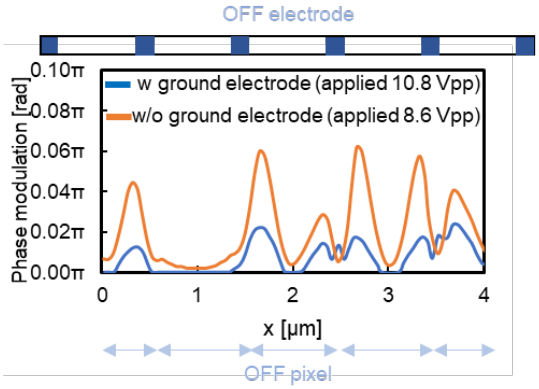

(c)

Fig. 13 Analysis results of phase-modulation distribution. (a) Cross-section {1}, (b) cross-section {2}, and (c) expanded cross-section {2}

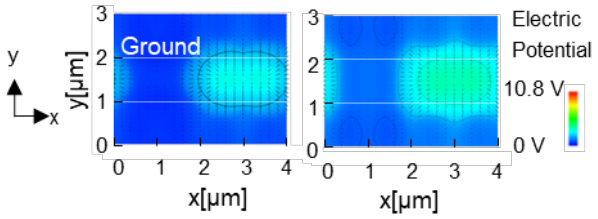

(a) (b)

Fig. 14 Analysis of the results of the electric potential and liquid crystal–alignment distribution (a) with and (b) without the ground electrode

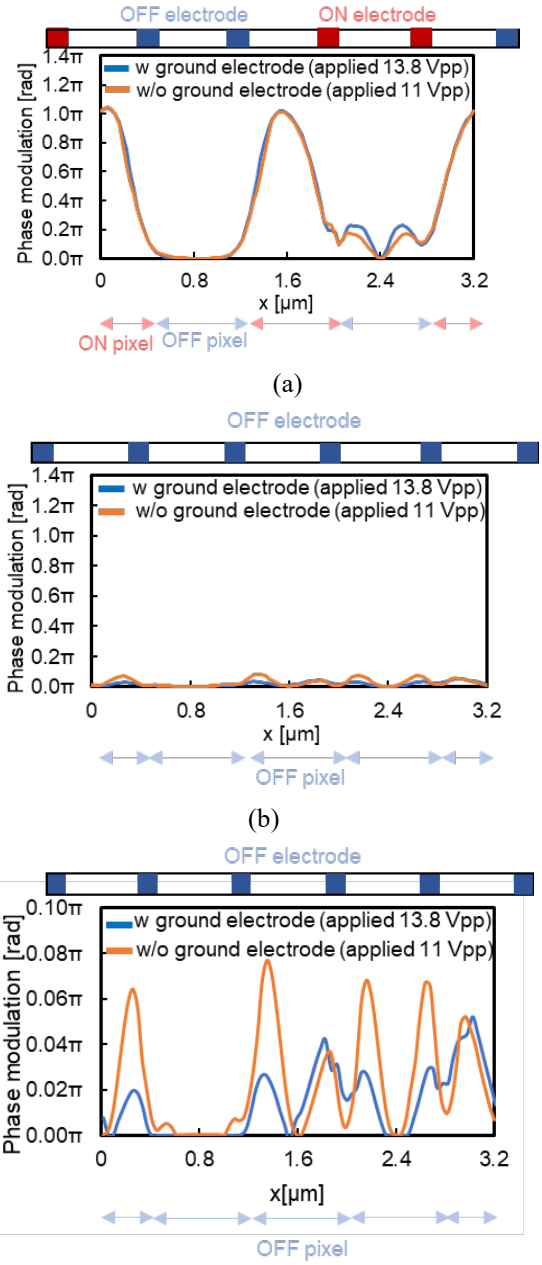

Fig. 15 Analysis results of the phase-modulation distribution: (a) cross-section {1}, (b) cross-section {2}, and (c) expanded cross-section {2}

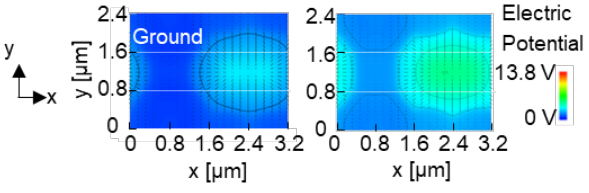

Fig. 16 Analysis results of the electric potential and liquid crystal–alignment distribution

(a) with and (b) without the ground electrode

while that with the ground electrode was 0.052π. Thus, the leakage is suppressed in this case using a ground electrode. However, pixel pitch of 0.8 μm condition leakage suppressing effect is reduced than pixel pitch of 1μm condition. As depicted in Fig. 16(a), in the presence of the ground electrode, electric potential does not spread to the upper and lower rows of the element in the in-plane observation plane {3}, resulting in a lower potential. This is similar to the results depicted in Fig. 14(a). However, as illustrated in Fig. 16(b), without the ground electrode, electric potential spreads to the upper and lower rows. Therefore, the ground electrode achieves leakage suppression in the element in the in-plane observation plane.

These results demonstrate that leakage is suppressed under the pitch conditions of 1 μm and 0.8 μm. In particular, devices with a pixel pitch of 0.8 μm can contribute to holographic viewing angles of 38 degrees by employing potential difference driving and a ground electrode. Thus, this pitch size is deemed feasible for repeatable production. To further reduce the pitch size, efforts will be focused on miniaturizing electrodes.

5. Conclusions

In this study, we introduced a pixel structure that integrates a lateral electric-field driving method based on a continuous potential-difference driving via lateral electrodes with a ground electrode for the practical implementation of electronic holographic displays. Employing this structure, we verified the independent driving capabilities of all pixels arranged in a 2D configuration. The results of this study show the suppression of electric-field leakage in 1 μm pixel pitch driving by measurement and in 0.8 μm pixel pitch suppression electric-field leakage.

Less than 1 μm pixel pitch is achieved for driven, which contributes to holography with 38 degrees human's effective field of viewing angle.

Acknowledgments

The authors would like to thank Professor Takahiro Ishinabe of Tohoku University and Assistant Professor Yosei Shibata of the Nagaoka University of Technology for their valuable discussions.

References

[1]D. Gabor, "A new microscopic principle," *Nature*, vol. 161, no. 4098, pp. 777–778, 1948.
[2]T. Kakue, T. Nishitsuji, T. Kawashima, K. Suzuki, T. Shimobaba, and T. Ito, "Aerial projection of three-dimensional motion pictures by electro-holography and parabolic mirrors," *Scientific Reports*, vol. 5, no. July, pp. 11750, 2015.
[3]D. Vettese, "Microdisplays: Liquid crystal on silicon," *Nature Photonics*,

vol. 4, no. 11. pp.752–754, 2010.
[4]Z. Zhang, Z. You, and D. Chu, "Fundamentals of phase-only liquid crystal on silicon (LCOS) devices," *Light: Science and Applications*, vol. 3, no. 10. pp. e213, 2014.
[5]Y. Isomae, Y. Shibata, T. Ishinabe, and H. Fujikake, "Design of 1-μm-pitch liquid crystal spatial light modulators having dielectric shield wall structure for holographic display with wide field of view," *Optical Review*, vol. 24, no. 2, pp. 165–176, 2017.
[6]H. Cheng, J. Yan, T. Ishinabe, and S. T. Wu, "Vertical field switching for blue-phase liquid crystal devices," *Applied Physics Letters,* vol. 98, no. 26, pp. 261102, 2011.
[7]T. Scheffer, and J. Nehring, "Twisted nematic and supertwisted nematic mode LCDs," *Liquid Crystals: Applications and Uses,* vol. 1, pp. 231–274, 1990.
[8]H. L. Ong, "Optical properties of general double layer twisted and supertwisted nematic liquid crystal displays," *Journal of Applied Physics*, vol. 64, no. 10, pp. 4867–4872, 1988.
[9]M. Oh-e, and K. Kondo, "Electro-optical characteristics and switching behavior of the in-plane switching mode," *Applied Physics Letters,* vol. 67, no. 26, pp. 3895–3897, 1995.
[10]Y. Isomae, Y. Shibata, T. Ishinabe, and H. Fujikake, "Design of 1-μm-pitch liquid crystal spatial light modulators having dielectric shield wall structure for holographic display with wide field of view," *Optical Review,* vol. 24, pp. 165–176, 2017.
[11]L. Yang, J. Xia, X. Zhang, Y. Xie, M. Kang, and Q. Zhang, "Fringing field suppression for liquid crystal gratings using equivalent capacitance configuration," *Japanese Journal of Applied Physics*, vol. 53, no. 10, 2014.

Hiroto Tochigi received the B.E. degree from Tohoku University, Sendai, Japan, in 2022. Now, he is a graduate student in the Department of Electronic Engineering, Graduate School of Engineering, Tohoku University. He is engaged in the design of high-resolution liquid-crystal devices for electronic holography. He received the Outstanding Poster Paper Award from IDW in 2023.

Masakazu Nakatani received his M.S. in Engineering from the Nara Institute of Science and Technology (NAIST) in March 2010 and Ph.D. in Engineering from the Nagaoka University of Technology in December 2020. From 2010–2016, he worked in Clean Venture 21, a low-concentration photovoltaics venture company, as a researcher; from 2020–2022, he worked as a postdoctoral researcher at Osaka University, studying light control by cholesteric liquid crystals. In February 2023, he joined the Graduate School of Engineering, Tohoku University as an Assistant Professor.

Ken-ichi Aoshima received B.S. in Physics from Chiba University, Japan, in 1990 and Ph.D. in Engineering at the Nagaoka University of Technology. He worked for Fujitsu laboratory Ltd. from 1990 to 2003. He also worked at Stanford University as a visiting scholar from 2000 to 2002, where he started studying spintronics. He moved to the Japan Broadcasting Corporation (NHK) in 2003. Since then, he has been working on spintronics and optical devices.

Mayumi Kawana received the B.S. and M.S. degrees in Applied Physics from the Tokyo University of Science in 2000 and 2002, respectively. In 2002, she joined the Japan Broadcasting Corporation (NHK). Since then, she has been at NHK STRL. She has been working on a spatial light modulator for holography.

Yuta Yamaguchi received the B.E., M.E., and Ph.D. degrees in Electronic and Information Engineering from the Tokyo University of Agriculture and Technology in 2015, 2017, and 2020, respectively. In 2020, he joined the Japan Broadcasting Corporation (NHK). Since then, he has been at NHK STRL. He has been working on a liquid-crystal spatial light modulator.

Kenji Machida received the M.S. degree in Materials Science and Engineering from Hiroshima University, Hiroshima, Japan, in 1993 and Ph.D. degree in Electronics and Information Engineering from the Tokyo University of Agriculture and Technology, Tokyo, Japan, in 2006. In 1993, he joined the Japan Broadcasting Corporation (NHK). Since 1995, he has been engaged in research on magnetic recording, spintronics, and optical devices at NHK STRL.

Nobuhiko Funabashi received the B.E., M.E., and Ph.D. degrees in Physical Electronics from the Tokyo Institute of Technology in 1999, 2001, and 2011, respectively. In 2001, he joined the Japan Broadcasting Corporation (NHK). Since then, he has been at NHK STRL. He has been working on spintronics and optical devices.

Hideo Fujikake received M.E and Ph.D. degrees from Tohoku University, Japan, in 1985 and 2003, respectively. In 1985, he joined the Japan Broadcasting Corporation (NHK). During 1988–2012, he was with NHK Science and Technology Research Laboratories. Since 2012, he has been a professor at the Department of Electronic Engineering, Tohoku University. He received Best Paper Award from the Institute of Electronics, Information and Communication Engineers (IEICE) in 2001, Best Paper Award from the Japanese Liquid Crystal Society (JLCS) in 2001 and 2015, Niwa-Takayanagi Best Paper Awards from the Institute of Image Information and Television Engineers of Japan (ITE) in 2003 and 2009, and Electronics Society Award from IEICE in 2013. His current interest focuses on flexible liquid-crystal displays. He also served as a General Vice Chair in International Display Workshops in 2015–2016, a Japan Chapter

Chair in IEEE Consumer Electronics Society in 2012–2014, and a Vice President of Japanese Liquid Crystal Society in 2015–2016. He is an IEICE fellow since 2015 and ITE fellow since 2016.